Fourier-transform-limited laser pulses tunable in wavelength and in duration (400-2000 ps)

Schiemann, S.; Hogervorst, W.; Ubachs, W.M.G.

published in
IEEE Journal of Quantum Electronics
1998

DOI (link to publisher)
10.1109/3.661446

document version
Publisher's PDF, also known as Version of record

Fourier-Transform-Limited Laser Pulses Tunable in Wavelength and in Duration (400–2000 ps)

Stephan Schiemann, Wim Hogervorst, and Wim Ubachs

***Abstract*—A combined system of an injection-seeded pulsed dye amplifier and a pulse compressor based on stimulated Brillouin scattering (SBS) is investigated. It allows for the generation of powerful pulses both tunable in wavelength and in duration. Online tuning of the pulse duration is possible due to the dependence of SBS compression on input energy. A range of 400–2000 ps at up to 100 mJ output energy is demonstrated. The output pulses are temporally and spectrally resolved to investigate the properties of this system. Coherent nearly Fourier-transform-limited pulses of variable pulse duration in the extreme ultraviolet (UV) are produced employing harmonic conversion. As an application of such pulses a single rotational line of H_2 at 98-nm wavelength is excited, demonstrating that the system may be used for laser-spectroscopic studies to simultaneously gain spectral as well as dynamical information.**

***Index Terms*— Brillouin scattering, dye lasers, optical pulse compression, optical pulses, pulse compression methods, pulsed lasers.**

I. Introduction

In LASER spectroscopy, structural and dynamical information can be extracted from both frequency- and time-domain measurements. Usually structural information is derived from high-resolution measurements in the frequency domain, for which narrow-bandwidth lasers are used. Dynamical information is deduced from time-domain measurements, for which short-pulse lasers are applied. Nonetheless, both types of information are entirely contained in each domain: lifetimes can be extracted from high-resolution spectral data via line broadening studies, while energy-level structures may follow from quantum beat experiments in the time domain [1]. Most information can be derived, if Fourier-transform (FT)-limited pulses are applied, in which the product of frequency uncertainty (bandwidth) and temporal uncertainty (pulse duration) is minimized. Also, optimum phase control of the emitted radiation is obtained. In present-day laser-based investigations, these coherence properties are more and more considered in combination with demand on flexible wavelength tunability and on variable pulse duration.

Mode-locked lasers almost automatically fulfill the FT limitation but only generate pulses with durations below 100 ps. Q-switched lasers generate pulses in the nanosecond regime instead, and the FT condition is approached, if narrow-band injection seeding is employed. In the present paper, we report on efficient temporal compression of the output of a wavelength-tunable pulsed dye amplifier into the range of 400–2000 ps. A pulse compressor, based on stimulated Brillouin scattering (SBS) in liquids, to be referred to as the "compact generator-amplifier setup" (CGAS) and introduced in a previous study in [2], is applied. It was demonstrated that high-energy FT-limited laser pulses from a nontunable, frequency-doubled Nd:YAG laser can be compressed from 5 ns down to 300 ps with energy conversion efficiency of 90% using the CGAS. The present paper deals with an important extension of this work in two directions, namely the compression of wavelength-tunable radiation and the generation of pulses with a variable duration.

The temporal and spectral characteristics of the output of the combined laser and compressor system are investigated in detail. A prescription on how to efficiently generate wavelength-tunable pulses with durations variable in the nanosecond to subnanosecond time domain could be deduced. The results are supported by numerical simulations of the SBS process in the specific cell arrangement; good agreement with observations is obtained. The SBS-generated pulses can be applied in a variety of laser spectroscopic experiments. We demonstrate that they can be frequency-doubled, subsequently up-converted into the extreme ultraviolet (XUV)-domain, and used for the excitation of a highly excited state of molecular hydrogen at 98 nm.

II. Experimental Characterisation of the Laser System

A. Experimental Setup

The laser and detection system are depicted in Fig. 1. The laser system consists of a nanosecond pulsed dye amplifier (PDA) and a pulse compressor, based on SBS in liquids. FT-limited pulses of duration $\tau_p = 5.5$ ns are generated by pulsed amplification of radiation from a CW ring dye laser Spectra-Physics 380 D (output 700 mW, 1 MHz bandwidth). The CW radiation is transmitted through a single-mode fiber link and amplified in three consecutive stages of dye cells, pumped by the second-harmonic of a single-mode Nd:YAG-laser Spectra-Physics GCR 5 (10 Hz repetition rate, 740 mJ output energy at 532 nm). Details of this amplifier system are described in [3]. Pulse energies up to 230 mJ in the wavelength range 589–592 nm are obtained from a dye mixture of Rhodamine 101 and Sulforhodamine B. Longitudinal pumping of the second and third dye amplifier stages of the PDA produces a spatial beam

Manuscript received May 6, 1997; revised November 21, 1997. This work was supported by the Training and Mobility of Researchers program of the European Union under Contract ERB4001GT952 808.

The authors are with the Laser Centre Vrije Universiteit, Amsterdam, The Netherlands.

Publisher Item Identifier S 0018-9197(98)01779-5.

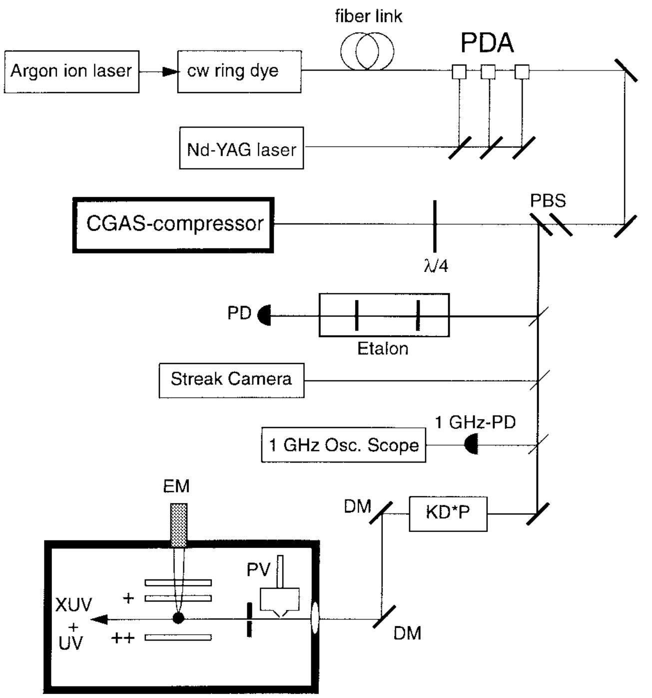

Fig. 1. Schematic of the experimental setup. It consists of the PDA including the cw seed laser and a fiber link, the SBS-based pulse compressor (CGAS) and the detection devices. The setup for a spectroscopic application is shown as well: the CGAS output is frequency-doubled in a KD^*P crystal. The resulting UV radiation is isolated by two dichroic mirrors (DM) and focused into a gas jet, produced with a pulsed valve (PV). The generated XUV radiation is applied for 1 XUV + 1 UV resonant photoionization of H_2 in a molecular beam, which perpendicularly intersects the light beams. Ions are detected with an electron multiplier (EM).

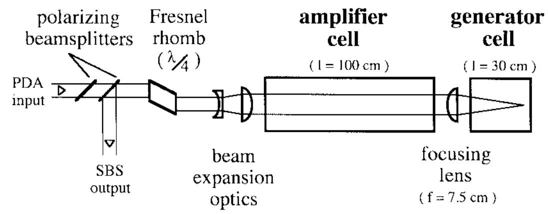

Fig. 2. Schematic of the SBS pulse compressor (CGAS, [2]). Two consecutive polarizing beam splitters are necessary to sufficiently isolate the PDA laser (not shown) from backscattered Brillouin radiation. Beam expansion optics can be used for adjusting the pump energy density in the amplifier cell at constant energy of the input pulses (not applied in this paper).

profile of diameter 9 mm with a nearly Gaussian intensity distribution.

The PDA pulses are launched into the CGAS, a two-cell SBS compressor characterized in [2]. In Fig. 2, details of this compressor type are shown. All cell windows and the focusing lens are antireflection-coated; liquid methanol is chosen as Brillouin medium in both cells (cell diameter 4 cm each), filtered to minimize solid impurities in the liquid. The operation of the CGAS may be summarized as follows: a short focal-length lens (f = 7.5 cm) in front of the generator cell (30 cm length) is used to create stimulated Brillouin radiation from the leading edge of the PDA pulse. The backscattered beam seeds the amplifier cell (100 cm length) located at a minimum distance from the generator. During the sustained interaction of pump and Brillouin radiation in the amplifier cell, the SBS pulse experiences strong intensity amplification and a substantial temporal reshaping. Its duration drops below the acoustic phonon lifetime in the SBS medium and the CGAS approaches its reflectivity of nearly 100%. Beam expansion optics can be used for adjusting the pump energy density in the amplifier cell at constant input energy (not applied in this work). The Brillouin radiation is separated from the pump radiation by means of its polarization state, using a combination of a Fresnel rhomb and polarizing beam splitters. Two consecutive polarizing beam splitters are required to sufficiently isolate the PDA laser from the backscattered pulses. As a consequence, the maximum reflectivity of the compressor system including all reflection losses reduces to 75% at 100% internal SBS conversion efficiency. The wavelength tunability of the system is determined by the tunability range of the CW laser (570–615 nm in case of operation with Rhodamine 6G) and by the tunability range of the specific dye mixtures in the PDA amplifier stages (580–600 nm in case of operation with a mixture of Rhodamine 101 and Sulforhodamine B). The entire wavelength interval 550–650 nm is accessible with the present setup by choosing the proper dye combinations. The range of continuous tunability is determined by the transmission function of the polarizing beam splitters. In the following experiments, beam splitters of optimum isolation around 591-nm wavelength are used.

For a temporal analysis of the compressed pulses, both a streak camera of type Hadland Imacon 500 and a combination PIN photodiode (bandwidth 1 GHz) plus digital oscilloscope (1-GHz analogue bandwidth, 5-Gs/s sampling rate) are applied. For a spectral analysis of the compressed pulses, an etalon of FSR 750 MHz is used.

B. Temporal Laser Pulse Characteristics

The CGAS compressor is adjusted to generate SBS pulses of minimum duration at 145 mJ PDA input energy. In Fig. 3, a streak camera recording of such a pulse of 400 ps (FWHM of intensity) duration is shown. Table I lists SBS pulse durations as a function of the CGAS input energy. The temporal profiles are recorded with the photodiode/oscilloscope detection system by integrating over the centeral part of the beam (diameter 2.5 mm). The pulses of input energy 80 and 100 mJ are generated at a PDA wavelength of 591.9 nm, all others at 589.9 nm.

The temporal resolution of the detection system is limited to 500 ps—this value was determined by monitoring femtosecond laser pulses. Corrected pulse durations are obtained by deconvoluting the oscilloscope data with these pulses. Nonetheless, at durations below 500 ps, this method becomes imprecise. It is sensitive to the actual shapes of both the reference and the measured pulse. Since the measured PDA pulse shapes are of nonperfect Gaussian type, the corrected pulse duration values are overestimated by the deconvolution procedure. As a consequence, the FWHM-value of a 400-ps pulse (streak camera measurement) at 145-mJ input energy is derived to 492 ± 50 ps from the oscilloscope data. In Fig. 4, a graphical representation of the data for corrected pulse durations as a function of CGAS input intensity is given. The results of a

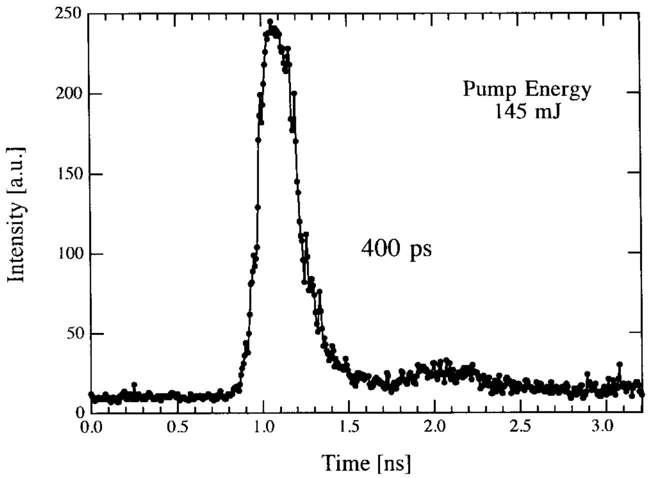

Fig. 3. Streak camera image at 10-ps resolution of SBS output at 145-mJ input energy. Only the central part of the beam (diameter 2.5 mm) is exposed to the camera. Shown is one line of the 2-D image digitized at 8-bit intensity resolution and at 6.5-ps time steps. Due to a nonlinear intensity response of the detection system, the "half-maximum" intensity level corresponds to 20% of the peak intensity, determined experimentally with a 50% attenuator.

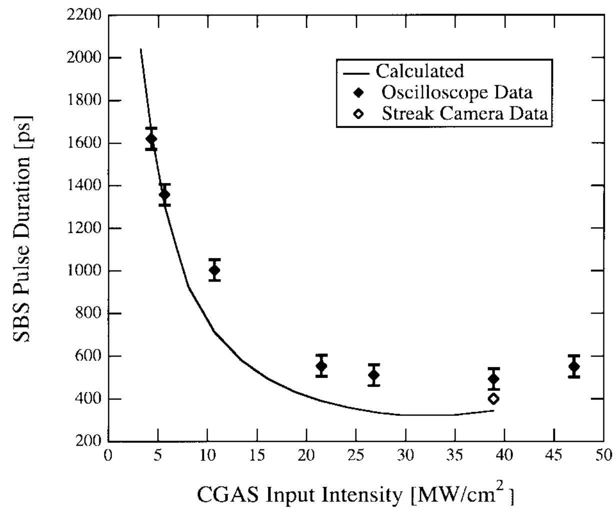

Fig. 4. Measured duration of compressed pulses plotted against the CGAS input intensity. Values are corrected for the limited resolution of the detection system. All data are taken from the central part of the beam (diameter 2.5 mm). Pulses of input intensity 26.8 and 21.5 MW/cm^2 are generated at 591.9-nm PDA wavelength, all others at 589.9 nm.The solid line represents a theoretical prediction generated by a numerical simulation of the compression process.

TABLE I
DURATIONS OF COMPRESSED PULSES AT VAROIUS CGAS INPUT ENERGIES

input energy [mJ]	input intensity [MW/cm^2]	measured SBS pulse duration [ps]	corrected SBS pulse duration [ps]
175	47.0	726	551
145	38.9	668	492
100	26.8	680	511
80	21.5	725	553
40	10.7	1020	1003
21	5.6	1380	1358
16	4.3	1642	1621

theoretical prediction are included in the graph as well. Details of this calculation are discussed in Section III-A.

At input energies larger than 145 mJ, the amplifier cell itself starts operating as an SBS mirror [2], giving rise to diffuse emission patterns in the spatial profile of the reflected beam and to a broadening in the temporal profile. At energies below 145 mJ, the duration of the SBS pulses increases with decreasing energy; the spatial profile remains unchanged.

C. Spectral Laser Pulse Characteristics

A spectral analysis for SBS pulses in the range of 500–2000 ps with an etalon (FSR 750 MHz) is made as well. The results are shown in Fig. 5. The spectral resolution of the etalon is calibrated by monitoring the CW laser output [Fig. 5(a)]: transmission fringes have a 20-MHz width (FWHM), corresponding to a finesse of 37.5. Another trace shows the spectrum of the PDA output before it is coupled into the SBS compressor [Fig. 5(b)]. The spectra (b)–(g) are generated in the following way: during continuous firing of the PDA at 10 Hz repetition rate and detection of the etalon transmission level with a photodiode, the wavelength of the CW laser is slowly scanned over approximately 0.15 cm^{-1}, starting at $\lambda = 591$ nm center wavelength. An interval of 1 FSR of each etalon trace is generated from 252 consecutive laser shots, including averaging over four laser shots at each data point of the spectrum. SBS pulses of various duration are generated by attenuating the energy of the pump pulses entering the CGAS compressor. This is realized by reducing the energy of the Nd:YAG pump laser source and by placing dielectric or absorbing filters into the laser beam. The widths $\Delta\nu_E$ (FWHM of intensity) of the observed etalon transmission fringes are derived by fitting the profiles of Fig. 5 to series of sine-square lineshapes.

III. DISCUSSION

A. Temporal Analysis

The CGAS compressor emits pulses of duration τ_s which are continuously variable within the following limits: the maximum is given by the pump pulse duration τ_p, the minimum $\tau_s^{\min}$ relates to the phonon lifetime τ_B in the liquid Brillouin medium. The relation $\tau_s^{\min} < \tau_B$ holds in general; for more detailed information, see [4] and [5]. At shorter input wavelengths shorter pulses can be generated. In practice, $\tau_s^{\min}$ is limited to the 100-ps range. The streak camera measurement of $\tau_s^{\min} = 400$ ps in the present setup, as presented in Fig. 3, is in accordance with the relation above, since for methanol the phonon lifetime is $\tau_B = 462$ ps. This value is based on data from [6], corrected to $\lambda_p = 591$ nm using the wavelength dependence given in [7]. The extraction of minimum pulse duration at a specific input energy necessitates proper adjustment of the laser beam diameter on the CGAS. For this purpose, beam expansion optics can be used, cf.

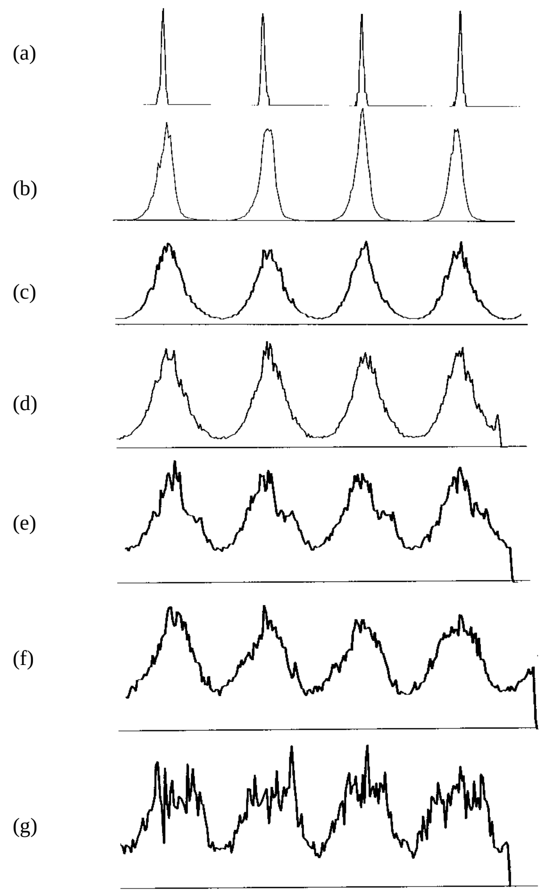

Fig. 5. Measured etalon traces (FSR 750 MHz) of (a) CW radiation from the ring dye laser, (b) uncompressed PDA laser pulses, and (c)–(g) pulses generated in the CGAS compressor at various compression factors. The widths $\Delta\nu_E$ (FWHM of intensity) of the transmission fringes are derived from fitting and averaging over several free spectral ranges each: (a) $\Delta\nu_E = 20$ MHz, (b) $\Delta\nu_E = 95$ MHz, $\tau = 5.5$ ns, (c) $\Delta\nu_E = 245$ MHz, $\tau = 1900$ ps, (d) $\Delta\nu_E = 270$ MHz, $\tau = 1330$ ps, (e) $\Delta\nu_E = 380$ MHz, $\tau = 983$ ps, (f) $\Delta\nu_E = 435$ MHz, $\tau = 614$ ps, and (g) $\Delta\nu_E = 500$ MHz, $\tau = 501$ ps.

Fig. 2. In the present experiment, the CGAS is operated at $P_{\max} = 145$-mJ input energy for highest compression without using these optics. Table I and its graphical representation in Fig. 4 illustrate this choice: with increasing pump intensity the pulse duration decreases until the minimum is reached shortly below 40 MW/cm^2. At higher intensity, the CGAS amplifier cell itself starts operating as an SBS mirror and the pulse duration again increases. The points in Fig. 4 were measured for different wavelengths (591.9 versus 589.9 nm). Since the phonon lifetime only marginally depends on wavelength, the experimental data and the theoretical curve can be compared without reference to specific wavelength.

In addition to the measured data, Fig. 4 depicts the dependency of τ_s on pump intensity as derived from a numerical simulation of the compression process in the CGAS. This simulation is based on a model of Brillouin scattering presented in [2] and summarized in the Appendix. At low intensities, an increase in CGAS input energy results in a steep shortening of the pulse duration, whereas near to the minimum of the curve τ_s is relatively insensitive to intensity variations in a wide range. The calculated curve ends at 40 MW/cm^2 because at higher intensities distinct multiple-peak structures in the temporal pulse profile appear [2], thus preventing a unique assignment of τ_s. At nanosecond durations, the experimental τ_s values precisely follow the numerical curve; at $\tau_s < 1$ ns values are slightly higher. This discrepancy may be ascribed to the inaccurate deconvolution process, required to correct for the limited resolution of the photodiode in this temporal range.

A prescription for generating FT-limited pulses of variable duration is as follows. Even minor deviations from $P_{\max}$ toward lower values already result in an increase of τ_s of the order of several hundreds of picoseconds. A shift into the nanosecond regime, however, needs stronger input energy attenuation. The acceptable minimum level of CGAS reflectivity determines the *useful* tunability range in pulse duration τ_s: starting from 60% reflectivity at $\tau_s = 400$ ps, corresponding to 85% internal Brillouin conversion inside the glass cells, the value drops to 40% at $\tau_s = 1600$ ps. It is mainly induced by a loss of energy density in the pump beam focus in the CGAS generator cell. An increasing fraction of energy at the leading edge of the PDA pulse is unused in the focus before the SBS threshold is exceeded and the compressor starts reflecting. High conversion efficiency at $\tau_s > 1$ ns can simply be reestablished by choosing a shorter focal-length lens in front of the generator cell and by introducing a slightly smaller pump beam diameter into the CGAS. A different Brillouin medium of higher SBS gain such as acetone could be chosen as well. It depends on the application to decide whether pulse duration tunability by controlling the CGAS input energy is sufficient or that it needs a combined manipulation of input energy *and* optical components of the CGAS. On-line variations in the range $\tau_s^{\min} < \tau_s < \tau_s^{\min} +$ 400 ps at a high efficiency level are conveniently realized without optical setup changes. Nonetheless, such changes can be applied to extend the operational range of the combined system up to several hundreds of millijoules of output energy by shifting the compression maximum into this range.

B. Spectral Analysis

The results of a spectral analysis of the compressed pulses are shown in Fig. 5. For a pulse of Gaussian temporal profile and of constant phase, the product $p = \Delta\tau_{1/2}^I \cdot \Delta\nu_{1/2}^I$ is 0.44, if both the duration $\Delta\tau$ and the bandwidth $\Delta\nu$ are measured as FWHM values of the intensity data. Such a pulse is defined as Fourier-transform limited. Non-Gaussian or phase-fluctuating pulses generate values $p > 0.44$. A PDA laser pulse of duration 5.5 ns, if it is assumed to be FT limited and Gaussian, would correlate to a frequency bandwidth of 80 MHz. Fig. 5(b) depicts observed etalon transmission fringes of PDA pulses. The width of $\Delta\nu_E = 95$ MHz agrees well with the given estimate, considering the spectral resolution of the etalon of 20 MHz [cf. trace (a)].

An inspection of the widths $\Delta\nu_E$ of the SBS pulse transmission fringes [Fig. 5(c)–(g)] reveals an increase with decreasing pulse duration τ_s. Pulses of $\tau_s > 1$ ns are found to remain nearly FT limited after the compression process. Durations $\tau_s < 1$ ns are too short to be quantitatively analyzed due to loss of multipath interferences in the etalon of 10-cm

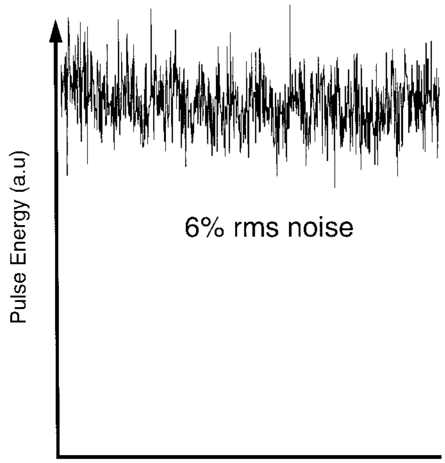

Fig. 6. Measured signal strength (integrated energy per pulse) of the compressor output (one data point per pulse), recorded at a CGAS input energy of 145 mJ. The pulse-to-pulse fluctuations are 6% rms.

mirror separation. However, based on theoretical as well as on experimental evidence (see Section IV) it is expected that also these subnanosecond pulses will be nearly FT-limited.

At decreasing pulse duration, a growth in signal noise on the fringes can be observed. This effect is not due to pulse-to-pulse fluctuations of the CGAS output energy, as was confirmed by simultaneously monitoring the signal strength (integrated energy per pulse) at the entrance of the etalon. In Fig. 6 a fraction of the data, recorded at a CGAS input energy of 145 mJ, is depicted. It proves a relatively low value of 6% rms energy fluctuations. Here the root-mean-square fluctuations are defined as

$$\Delta x_{\mathrm{rms}} = \frac{\sqrt{\sum_i (x_i - \overline{x})^2}}{\overline{x}}. \tag{1}$$

The noise effect in the etalon traces is ascribed to shot-to-shot variations in the spectral energy density or in the center frequency of the pulses. This leads to a different transmission signal in the 20-MHz frequency window of the etalon for each individual laser pulse.

IV. Spectroscopic Application of the Compressed Pulses

As an example of the application of SBS-compressed pulses from the combined PDA laser/CGAS compressor system here a demonstration experiment is reported. The experimental setup is shown in the lower part of Fig. 1. Pulses of 100-mJ energy and of 400-ps duration emitted from the CGAS at $\lambda = 589.5$ nm are frequency doubled in a KD^*P crystal, yielding a UV pulse energy of 13 mJ. The UV pulses are upconverted via third-harmonic generation in a pulsed xenon gas jet and used for 1 XUV + 1 UV photoionization of molecular hydrogen in a molecular beam. The applied excitation scheme of H_2 is described in detail in [8]. Spectral recordings are taken both with uncompressed output of the PDA and with compressed pulses from the CGAS. The CGAS is adjusted for maximum compression—pulses of approximately 400-ps duration generated in the SBS medium methanol. In Fig. 7, $1 + 1$ REMPI spectra of the singly resolved R(1) rotational line of the $B^1\Sigma_u^+ - X^1\Sigma_g^+$ (10, 0) band of H_2 for both types of pulses are shown. Markers of a calibrated monitor etalon (FSR 149 MHz) are used to determine the linewidth of the resonance [Fig. 7(c)].

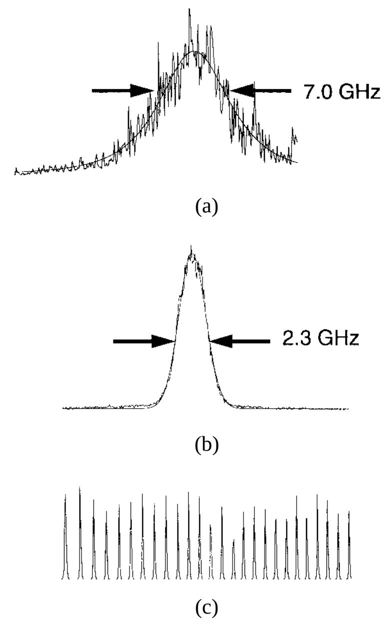

Fig. 7. Measured spectral line profiles, via 1 XUV + 1 UV photoionization, for the R(1) transition in the $B^1\Sigma_u^+ - X^1\Sigma_g^+(10,0)$ band of H_2: (a) detected with compressed CGAS pulses after upconversion to XUV, and (b) detected with uncompressed PDA laser pulses after upconversion to XUV. Trace (c) shows monitor etalon frequency markers of 149-MHz separation recorded using the CW seed–laser radiation at 590 nm.

The spectral bandwidth of uncompressed PDA pulses after frequency doubling and third-harmonic generation is ≈250 MHz, determined in [9]. The linewidth of the H_2 resonance monitored with these pulses is 2.3 GHz [see Fig. 7(b)]. It is entirely due to Doppler broadening in the free molecular jet. A spectrum of the rotational line scanned with compressed pulses is shown in Fig. 7(a), yielding a spectral width of 7.0 GHz. After correction of this profile for Doppler broadening the true bandwidth of the compressed XUV pulses is estimated to be $\Delta\nu^{XUV} = 6.0$ GHz. Without being able to measure the compressed pulses duration in the XUV, we estimate a reduction in duration from $\tau_s^{\mathrm{VIS}} = 400$ ps in the visible by a factor of $\sqrt{6}$ due to sixth harmonic conversion to $\tau_s^{\mathrm{XUV}} \approx 160$ ps in the XUV, assuming a Gaussian temporal profile. From this a product $\Delta\nu^{\mathrm{XUV}} \cdot \tau_s^{\mathrm{XUV}} = 1$ is derived, showing that the compressed XUV pulses are close to being FT limited.

V. Summary and Conclusion

In this paper, the output of a combined setup of an injection-seeded PDA and an SBS pulse compressor of CGAS type is experimentally investigated by measurements in the time and frequency domain. The temporal analysis demonstrates the potential of this system to provide on-line tunability in pulse duration in a range of 400–2000 ps without significant loss in output energy. The high conversion efficiency and the ease of pulse duration control are attractive features of the CGAS compressor. The experiments were performed at a maximum of 100-mJ output energy, but it follows from the CGAS principle that an extension to several hundreds of millijoule energy is feasible. Parameters to control the pulse duration and to optimize the reflectivity are the CGAS input energy, the focal-length of the focusing lens, the beam diameter in the CGAS amplifier cell, and the SBS gain.

As a practical application of the pulses from the PDA/CGAS combination, the detection of a rotational line of molecular hydrogen in the XUV at 98-nm wavelength is presented. It shows that also wavelength-tunable pulses of variable pulse duration in the extreme ultraviolet can be generated and spectroscopically applied.

APPENDIX
NUMERICAL MODEL OF BRILLOUIN SCATTERING

The results of numerical simulations discussed in Section III-A are derived from a model of Brillouin scattering presented in [2]. This model is based on equations, describing the coupling of both radiation fields (the incident pump field E_p and the created Stokes field E_s) with the acoustic matter-density field ρ in the liquid [6], [7]

$$\begin{aligned} \frac{n}{c}\frac{\partial E_p}{\partial t} + \frac{\partial E_p}{\partial z} &= i g_1 \rho E_s \\ \frac{n}{c}\frac{\partial E_s}{\partial t} - \frac{\partial E_s}{\partial z} &= i g_1 \rho^* E_p \\ \frac{\partial \rho}{\partial t} + \frac{1}{2}\Gamma_B \rho &= i g_2 E_p E_s^*. \end{aligned} \tag{2}$$

The parameter $\Gamma_B = 1/\tau_B$ represents the phonon relaxation rate and γ_e the electrostrictive coupling constant. The photon-phonon coupling constants g_1, g_2 are defined as

$$g_1 = \frac{\gamma_e \omega_p}{4nc\rho_0} g_2 = \frac{\gamma_e k_B^2}{16\pi\omega_B} \tag{3}$$

with k_B, ω_B the wavevector and frequency of the phonon, ρ_0 the average density, and n the refractive index of the medium. A quantity usually applied to characterize an SBS medium is its steady-state SBS gain g_B, which is connected to g_1, g_2 by the relation

$$g_B = \frac{\gamma_e^2 \omega_p^2}{nvc^3 \rho_0 \Gamma_B} = g_1 g_2 \frac{n}{c}\frac{32\pi}{\Gamma_B}. \tag{4}$$

For methanol $g_B = 0.013$ cm/MW, $\tau_B = 462$ ps and $\omega_B = 3.141 \cdot 10^{10}$ s^{-1} are derived from [6], extrapolated to $\lambda_p = 591$ nm. All remaining parameters are taken from [10]. The model assumes a circular spatial beam profile of constant intensity. To approximate the Gaussian distribution in the experiments, a spatial beam diameter of 6.5 mm in the calculations is chosen at the same pulse energy level.

ACKNOWLEDGMENT

The authors wish to thank I. Velchev for his assistance during the measurements.

REFERENCES

[1] W. Demtröder, *Laser Spectroscopy*. Berlin, Germany: Springer-Verlag, 1996.
[2] S. Schiemann, W. Ubachs, and W. Hogervorst, "Efficient temporal compression of coherent ns-pulses in a compact SBS generator-amplifier setup," *IEEE J. Quantum Electron.*, vol. 33, pp. 358–366, 1997.
[3] K. S. E. Eikema, W. Ubachs, W. Vassen, and W. Hogervorst, "Lamb shift measurement in the 1 ^{1}S ground state of helium," *Phys. Rev. A*, vol. 55, pp. 1866–1884, 1997.
[4] M. A. Davydov and I. N. Koshevnikova, "Laser-pulse compression by stimulated Brillouin scattering in liquids," *Phys. Lett. A*, vol. 127, pp. 345–346, 1988.
[5] V. A. Gorbunov, S. B. Papernyi, V. F. Petrov, and V. R. Startsev, "Time compression of pulses in the course of stimulated Brillouin scattering in gases," *Sov. J. Quantum Electron.*, vol. 13, pp. 900–905, 1983.
[6] W. Kaiser and M. Maier, "Stimulated Rayleigh, Brillouin, and Raman spectroscopy," in *Laser Handbook*, F. T. Arecchi and E. O. Schulz-Dubois, Eds. Amsterdam, The Netherlands: North Holland, 1972, vol. 2, pp. 1077–1150.
[7] R. W. Boyd, *Nonlinear Optics*, New York: Academic, 1992.
[8] P. C. Hinnen, S. Stolte, W. Hogervorst, and W. Ubachs, "Sub-Doppler laser spectroscopy of H_2 and D_2 in the range 91–98 nm," *Can. J. Phys.*, vol. 72, pp. 1032–1042, 1994.
[9] W. Ubachs, K. S. E. Eikema, W. Hogervorst, and P. C. Cacciani, "A narrowband tunable XUV-laser source for lifetime measurements and precision spectroscopy," *J. Opt. Soc. Amer. B*, vol. 14, pp. 2469–2476, 1997.
[10] R. C. Weast and M. J. Astle, Eds., *CRC Handbook of Chemistry and Physics*. Boca Rato, FL: CRC Press, 1983.

Stephan Schiemann was born in Berlin, Germany, on June 21, 1964. He received the Diploma in physics and the Ph.D. degree from the University of Kaiserslautern, Germany, in 1989 and 1994, respectively.

Presently, he is working as a Post-Doctoral Research Fellow at the Vrije Universiteit Amsterdam, The Netherlands. His research interests include coherent light–matter interactions, nonlinear optical processes, and the generation of coherent soft X-ray radiation.

Wim Hogervorst has been a Professor in Atomic and Laser Physics at the Vrije Universiteit, Amsterdam, The Netherlands, since 1986. He is the founder of the interdisciplinary Laser Centre, which opened in 1992, and he is the leader of a research group whose main areas of interest include laser spectroscopy of atoms and molecules, nonlinear optical processes, laser cooling and trapping of atoms, and solid-state laser development.

Wim Ubachs received the Drs. degree from the University of Nijmegen for a study in solid-state physics. He received the Dr. degree from the same university in 1986 for high-resolution laser spectroscopic studies of diatomic hydrides.

As a Post-Doctoral Research Fellow, he worked at the Dalian Institute of Chemical Physics (China) and the Department of Chemistry at Stanford University. Since 1988, he has been a Lecturer of Physics at the Vrije Universiteit Amsterdam, where his activities are aimed at the generation and spectroscopic application of coherent and tunable extreme ultraviolet radiation.